The FEBS Journal

FEBS PRESS science publishing by scientists

Membrane insertion mechanism and molecular assembly of the bacteriophage lysis toxin ΦX174-E

Julija Mezhyrova[1], Janosch Martin[2], Oliver Peetz[2], Volker Dötsch[1], Nina Morgner[2], Yi Ma[3,4] and Frank Bernhard[1]

1 Institute of Biophysical Chemistry and Center for Biomolecular Magnetic Resonance, Goethe University, Frankfurt am Main, Germany
2 Institute of Physical and Theoretical Chemistry, Goethe University, Frankfurt am Main, Germany
3 School of Biology and Biological Engineering, South China University of Technology, Guangzhou, China
4 Guangdong Provincial Key Laboratory of Fermentation and Enzyme Engineering, South China University of Technology, Guangzhou, China

Keywords
cell-free expression; molecular switch; nanodiscs; peptide antibiotics; phage lysis proteins

Correspondence
F. Bernhard, Institute of Biophysical Chemistry and Center for Biomolecular Magnetic Resonance, Max von Laue Str. 9. Goethe University, Frankfurt am Main 60438, Germany
Tel: +49 79 79829624
Y. Ma, School of Biology and Biological Engineering, South China University of Technology, Guangzhou 510006, People's Republic of China
Tel: +86 176 69556109
E-mail: bimayikobe@scut.edu.cn

Julija Mezhyrova and Janosch Martin contributed equally to this article.

(Received 17 August 2020, revised 23 October 2020, accepted 2 November 2020)

doi:10.1111/febs.15642

The bacteriophage ΦX174 causes large pore formation in *Escherichia coli* and related bacteria. Lysis is mediated by the small membrane-bound toxin ΦX174-E, which is composed of a transmembrane domain and a soluble domain. The toxin requires activation by the bacterial chaperone SlyD and inhibits the cell wall precursor forming enzyme MraY. Bacterial cell wall biosynthesis is an important target for antibiotics; therefore, knowledge of molecular details in the ΦX174-E lysis pathway could help to identify new mechanisms and sites of action. In this study, cell-free expression and nanoparticle technology were combined to avoid toxic effects upon ΦX174-E synthesis, resulting in the efficient production of a functional full-length toxin and engineered derivatives. Pre-assembled nanodiscs were used to study ΦX174-E function in defined lipid environments and to analyze its membrane insertion mechanisms. The conformation of the soluble domain of ΦX174-E was identified as a central trigger for membrane insertion, as well as for the oligomeric assembly of the toxin. Stable complex formation of the soluble domain with SlyD is essential to keep nascent ΦX174-E in a conformation competent for membrane insertion. Once inserted into the membrane, ΦX174-E assembles into high-order complexes via its transmembrane domain and oligomerization depends on the presence of an essential proline residue at position 21. The data presented here support a model where an initial contact of the nascent ΦX174-E transmembrane domain with the peptidyl-prolyl isomerase domain of SlyD is essential to allow a subsequent stable interaction of SlyD with the ΦX174-E soluble domain for the generation of a membrane insertion competent toxin.

Abbreviations
CF, cell-free; cv, column volume; D-CF, detergent based cell-free expression; DMPC, 1,2-dimyristoyl-sn-glycero-3-phosphocholine; DMPG, 1,2-dimyristoyl-sn-glycero-3-phospho-(1'-*rac*-glycerol); DOPG, 1,2-dioleoyl-sn-glycero-3-phospho-(1'-*rac*-glycerol); DPC, n-dodecyl phosphocholine; DTT, dithiothreitol; GDN, glycol-diosgenin; IMAC, immobilized metal affinity chromatography; IPTG, isopropyl-β-D-thiogalactopyranoside; L-CF, lipid based cell-free expression; LILBID, laser-induced liquid bead ion desorption; LMPG, 1-myristoyl-2-hydroxy-sn-glycero-3-phospho-(1'-*rac*-glycerol); ND, nanodisc; PBS, phosphate buffered saline; P-CF, precipitate forming cell-free expression; POPG, 1-palmitoyl-2-oleoyl-sn-glycero-3-phospho-(1'-*rac*-glycerol); RM, reaction mix.

Introduction

The discovery of penicillin in 1928 initiated the development of antibiotic therapies against bacterial infections. However, emerging microbial resistances became a serious threat to global public health in recent times and require search and development of new antibiotic agents. Single-stranded DNA or RNA phages lyse their bacterial hosts by small membrane-bound toxins. The prototype toxin from the ssDNA *Microviridae* group is the 91 amino acid protein ΦX174-E consisting of a proposed N-terminal transmembrane domain connected to a soluble domain [1]. The peptide is extremely toxic to bacteria and recombinant expression of ΦX174-E leads to rapid lysis of *E. coli*, which is characterized by large pore formation and subsequent release of cytoplasmic content [2–6].

Lysis by ΦX174-E resembles the mode of penicillin action, but the underlying mechanisms are different. ΦX174-E acts from the cytoplasmic site of the membrane and inhibits peptidoglycan precursor formation [1,6]. The presence of both ΦX174-E domains is essential for its lytic function. While the sequence of the proposed transmembrane domain is highly conserved, the soluble domain could also be replaced by some relatively unrelated proteins such as LacZ [7,8].

Two molecular targets of ΦX174-E have been identified. The interaction between MraY and ΦX174-E is a well-studied mechanism. An allosteric mode of inhibition was proposed, as toxin binding is noncompetitive for MraY substrates UDP-MurNAc-pentapeptide and undecaprenol phosphate [9,10]. The proposed interface of ΦX174-E and MraY includes residues within the transmembrane domains 5 and 9 of *E. coli* MraY [10]. A putative MraY binding motif at the very N terminus of ΦX174-E also present in other cationic peptides has been proposed, and a further possible role of the MraY interaction in promoting ΦX174-E membrane insertion was suggested [11]. The second target of ΦX174-E is the FKBP-type chaperone SlyD, and recessive mutations in the *slyD* gene were shown to prevent lysis. SlyD has a dual functionality and is composed of a peptidyl-prolyl *cis-trans* isomerization domain (P-domain) and an integrated IF domain (insertion into flap) having a postulated general chaperone activity [12]. Further studies indicated that SlyD is important for ΦX174-E stabilization [13].

MraY inhibition is crucial for ΦX174-E activity and subsequent lysis of the host cells caused by shortage of peptidoglycan precursors was proposed [9,10] However, several data indicate that bacterial lysis appears to be a more complex mechanism. A synthetic and lysis defective construct covering only the ΦX174-E N-terminal transmembrane domain still efficiently inhibits MraY [11,14]. Accordingly, pulldown studies revealed significant MraY binding to nonlytic ΦX174-E derivatives [8]. Furthermore, ΦX174-E binds distant from the active center of MraY and with a rather low affinity within the range of 0.5–0.8 μM [10,14,15]. This is in disagreement to the determined relatively low copy number of approx. 500–1000 ΦX174-E molecules sufficient to induce cell lysis [7,10]. Complementary to MraY inhibition, large 50–200 nm pores were observed by electron microscopy. The pores were preferentially located at areas of cell growth, which leads to the hypothesis of an active pore formation by high-order ΦX174-E oligomerization [4]. The soluble domain of ΦX174-E was proposed to become translocated through the cellular membranes to finally participate in a transmembrane tunnel, spanning the inner and outer membrane of Gram-negative bacteria.

Although to date *E. coli* is the most frequently used host for recombinant protein expression [16], it is limited in the production of toxins or membrane proteins. Several attempts have been made to produce ΦX174-E using cell-based systems, but efficient protocols allowing detailed functional analysis are still missing [10,14,17]. This work uses cell-free (CF) expression and nanodisc (ND) technology to address this problem. CF systems are independent of host viability and enable the preparative scale production of toxic proteins [18]. Furthermore, a specific expression background in processed bacterial lysates and the implementation of defined membrane systems such as NDs allow mechanistic studies of membrane insertion, oligomerization and molecular interactions of synthesized proteins [19–21].

This work provides new molecular details to refine the interaction of ΦX174-E with SlyD. We show that formation of a stable complex of SlyD with the soluble domain ΦX174-Esol is a prerequisite to keep the ΦX174-E toxin in a state, which is competent for membrane insertion. We propose a mechanistic model of ΦX174-E auto-inhibition, in which SlyD prevents the formation of an inactive conformation by initial interaction of its P-domain with the nascent transmembrane domain ΦX174-Epep, followed by stable complex formation of SlyD with the soluble domain ΦX174-Esol. In combination with native laser-induced liquid bead ion desorption (LILBID) mass spectrometry, we were the first to describe the high-order assembly of full-length ΦX174-E as well as of ΦX174-Epep after membrane insertion. Oligomeric assembly of the full-length toxin depends on the presence of the essential P21 residue in the transmembrane domain and is modulated in *cis* by the soluble domain.

Oligomerization of ΦX174-E adds a new characteristic to be considered in its lysis pathway, and the described strategy can furthermore serve as suitable platform to study similar toxins.

Results

CF and *in vivo* expression of ΦX174-E constructs

The full-length toxin ΦX174-E and the C terminally truncated derivative ΦX174-Epep spanning amino acid residues 1–37 were designed according to previous reports [14]. The ΦX174-Esol domain was fused to the C terminus of GFP in the GFP-Esol construct (Table 1). The constructs ΦX174-E-P21A and ΦX174-Epep-P21A contain a mutation in an essential proline residue of the transmembrane domain that completely abolishes lysis activity [8,30]. The peptides were first synthesized without any supplied hydrophobic environments. Synthesis yields of all constructs were in between 0.8 and 1.2 mg protein·mL^{-1} RM (Fig. 1A). The constructs ΦX174-E, ΦX174-Epep, ΦX174-E-P21A and ΦX174-Epep-P21A almost quantitatively precipitated in the absence of hydrophobic additives, and only a minor fraction of the putatively soluble GFP-Esol stayed in solution.

P-CF synthesized ΦX174-E and ΦX174-Epep precipitates could be completely solubilized in 0.75% 1-myristoyl-2-hydroxy-sn-glycero-3-[phospho-*rac*-(1-glycerol)] (LMPG) or to approx. 50% in 2% DPC. The co-translational solubilization of ΦX174-E and ΦX174-Epep in the D-CF mode was efficient in the presence of 0.4% of either Brij78, Brij35, or glyco-diosgenin (GDN). Brij35 was selected for further co-translational detergent solubilization experiments.

The potential toxicity of ΦX174-E and its dependency on SlyD was verified by complementary *in vivo* studies (Fig. 1B). Furthermore, the copy number of the synthesized protein was modulated by inducing the T7 RNA polymerase inhibitor T7 lysozyme with L-rhamnose. Growth curves of transformed *E. coli* Lemo21 (DE3) cells were recorded (a) with/without addition of L-rhamnose to suppress T7 RNA polymerase background expression before induction and (b) with/without co-expression of the chaperone SlyD from compatible plasmids (Fig. 1B). Cell lysis caused by ΦX174-E could not be suppressed upon addition of L-rhamnose, giving evidence that the required minimal copy number for cell lysis is relatively low. Co-expression of SlyD showed only a slight effect on the lysis onset, probably due to an already high titer of SlyD present in the cell background. As previously reported,

Table 1. CF synthesized constructs.

Construct	Amino acids[a]	Sequence[b]
ΦX174-E	1–91	MVRWTLWDTL AFLLLLSLLL PSLLIMFIPS TFKRPVSSWK ALNLRKTLLM ASSVRLKPLN CSRLPCVYAQ ETLTFLLTQK KTCVKNYVQK EGTGGWSHPQ FEK
ΦX174-E-P21A	1–91	MVRWTLWDTL AFLLLLSLLL ASLLIMFIPS TFKRPVSSWK ALNLRKTLLM ASSVRLKPLN CSRLPCVYAQ ETLTFLLTQK KTCVKNYVQK EGTGGWSHPQ FEK
ΦX174-Epep	1–37	MK RWTLWDTL AFLLLLSLLL PSLLIMFIPS TFKRPVSGTG GWSHPQFEK
ΦX174-Epep-P21A	1–37	MK RWTLWDTL AFLLLLSLLL ASLLIMFIPS TFKRPVSGTG GWSHPQFEK
GFP-Esol	33–91	MSKGEELFTG VVPILVELDG KLTLKFICTT GKLPVPWPTL VTTLTYGVQC FSRYPDHMKR HDFFKSAMPE GYVQERTISF KDDGTYKTRA EVKFEGDTLV NRIELKGIDF KEDGNILGHK LEYNFNSHNV YITADKQKNG IKANFKIRHN VEDGSVQLAD HYQQNTPIGD GPVLLPDNHY LSTQSVLSKD PNEKRDHMVL LEFVTAAGIT HGMDELYKHH HHHHLEVLFQ GPGSKRPVSS WKALNLRKTL LMASSVRLKP LNCSRLPCVY AQETLTFLLT QKKTCVKNYV QKEGTGGWSH PQFEK

[a]Amino acids of the ΦX174-E peptide in the corresponding constructs.; [b]Amino acid sequence of constructs, modifications within the ΦX174-E peptide parts and C-terminal StrepII/His_6-tags are underlined.

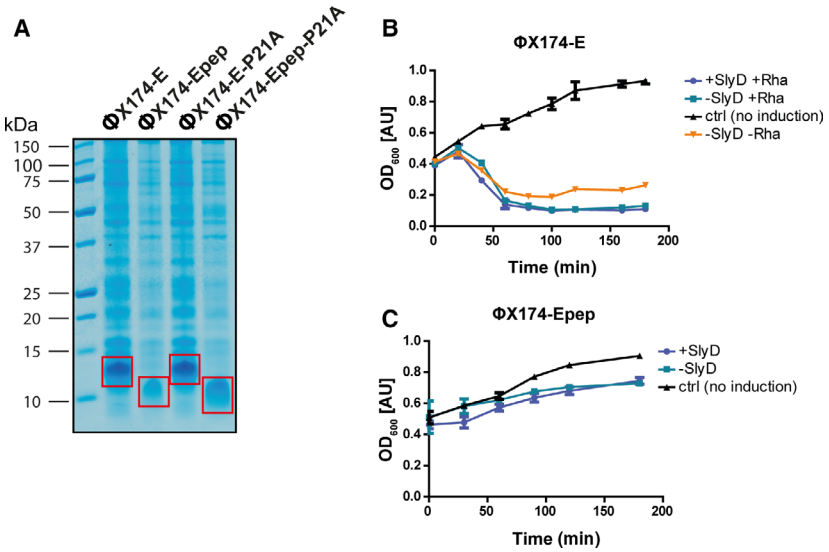

Fig. 1. P-CF expression of ΦX174-E and derivatives and *in vivo* lysis profiles of full-length ΦX174-E and truncated ΦX174-Epep. (A) All constructs were synthesized in P-CF mode. Samples were centrifuged after expression and pellets were resuspended in S30C buffer in the corresponding RM volume. For SDS/PAGE, 1.5 μL of samples was applied on discontinuous polyacrylamide gels, which were subsequently stained with colloidal Coomassie Brilliant Blue staining solution. Overexpression bands are framed by red boxes. Other bands appearing on the SDS/PAGE correspond to coprecipitated proteins from the A19 S30 lysate. The SDS/PAGE shows a representative P-CF expression of the toxins. (B, C) Growth curves were measured in *E. coli* Lemo21(DE3) cells with or without 500 μM L-rhamnose and co-expressed chaperone SlyD. Cells were induced at OD_{600} = 0.4. The curves show cell growth after induction, defined as t = 0. ΦX174-E lysis was not abolished in the presence of L-rhamnose, and SlyD co-expression may induce a slightly earlier lysis onset. ΦX174-Epep was not lytic to cells, independently of SlyD co-expression. Error bars represent the SEM from n = 3 independent biological repeats.

deletion of the soluble domain abolished any lysis ability (Fig. 1C) [7]. Expression of ΦX174-E in the mutant strain BL21(DE3)ΔSlyD/X did not result in any lysis (data not shown).

Co-translational insertion of ΦX174-E constructs into preformed ND membranes

For expression in the L-CF mode, CF reactions were supplied with increasing concentrations of preformed NDs containing membranes composed of either DMPG or DMPC lipids to analyze the efficiency of co-translational association/insertion of synthesized ΦX174-E and ΦX174-Epep (Fig. 2). Solubilization of the synthesized proteins resulting from their interaction with the ND bilayer was monitored via immunoblotting of the final supernatant and precipitate fractions. Both constructs were co-translationally solubilized to 80–90% at high ND concentrations. However, the kinetics of ND solubilization were different for the two proteins. Expression yields of full-length and truncated proteins were similar, and 80% of the truncated ΦX174-Epep was already solubilized in 20 μM NDs. In contrast, a fourfold higher ND concentration was necessary to solubilize 80% of the synthesized ΦX174-E. Considering the similar expression rate and the molecular weight difference between both, a significantly higher molar ratio of protein to ND is necessary to solubilize ΦX174-E if compared with its truncated derivative ΦX174-Epep. This result gives a first indication that the soluble domain of ΦX174-E might have a negative effect on its solubilization by NDs. In case of ΦX174-E, the negatively charged lipid head groups of DMPG supported solubilization, whereas no preference was detectable for ΦX174-Epep (Fig. 2). Using NDs preformed with DOPG or POPG having increased lipid chain length and flexibility did not show further improvement of solubilization (data not shown). NDs preformed with DMPG were therefore selected for further analysis of ΦX174-E membrane insertion.

Nascent ΦX174-E is solubilized by SlyD

Previous *in vivo* studies showed that the presence of the bacterial chaperone SlyD is essential for ΦX174-E toxicity [6,13,14]. For the characterization of molecular ΦX174-E/SlyD interactions in our CF system, SlyD was expressed in T7 express cells and purified via a

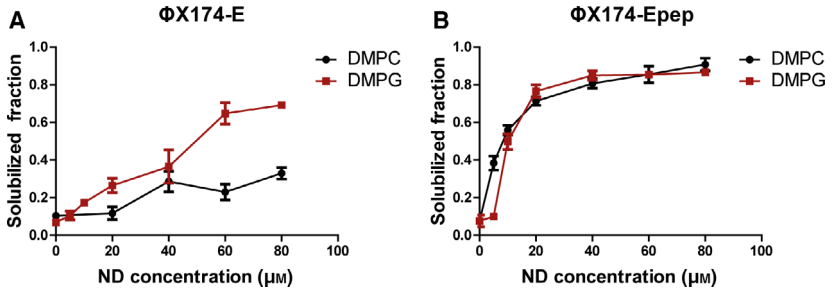

Fig. 2. Lipid dependent insertion of ΦX174-E and ΦX174-Epep into NDs. CF reactions were supplemented with different concentrations of NDs either composed of DMPC or DMPG lipids. After expression, samples were centrifuged and pellets were resuspended with S30C buffer in the respective RM volume. The fraction of solubilized ΦX174-E/ND complexes was determined by immunoblotting of pellet and supernatant. The combined signal from pellet and supernatant was normalized to 1. Error bars represent the SEM. (A) ΦX174-E titrations. The number of biological replicates for the respective data points is indicated in brackets (DMPC: 0 and 60 μM $n = 6$; 20 and 80 μM $n = 4$; 40 μM $n = 3$; DMPG: 5 and 60 μM $n = 6$, 20 and 40 μM $n = 4$, 0, 10 and 80 μM $n = 3$). (B) ΦX174-Epep titrations. The values were calculated from $n = 3$ replicates. For 5, 10, and 40 μM DMPC NDs, the number of repeats equals $n = 4$.

C-terminal His-tag as described in the methods section. According to previous proteomics analysis, our standard S30 CF lysate prepared from strain A19 may still contain a certain amount of functional SlyD [31]. We therefore analyzed the effects of supplied SlyD in CF reactions containing S30 lysates prepared from either the A19 strain or from a *slyD* negative BL21 strain [25]. The protein expression efficiency with the BL21(DE3)ΔSlyD/X lysate was approx. 50% the efficiency of A19 lysates, but allowed better control of the SlyD concentration in CF reactions.

If the CF reaction was adjusted to 100 μM SlyD at the beginning of ΦX174-E expression, up to 50% of synthesized ΦX174-E remained soluble even without the addition of hydrophobic compounds (Fig. 3). A similar, but less pronounced effect of co-translational solubilization by SlyD was observed with the lysis-deficient mutant ΦX174-E-P21A. The essential P21 residue in the transmembrane domain is proposed to be the target of the peptidyl-prolyl *cis-trans* isomerization domain of SlyD. However, the result shows that P21 is not essential for a SlyD/ΦX174-E complex formation, although the higher variation of the ΦX174-E-P21A solubilization efficiency may indicate a less stable interaction with SlyD. In contrast, almost no solubilization with SlyD was observed for the truncated derivative ΦX174-Epep (Fig. 3). Replacement of wild-type SlyD with the mutant SlyD-I42S-F132Y (= SlyD*) [32] containing an inactive P-domain abolished solubilization of ΦX174-E and ΦX174-E-P21A (Fig. 3). The co-translationally formed complex of SlyD and ΦX174-E was stable and both proteins were co-purified from the soluble fraction of CF reactions via the C-terminal StrepII-tag of ΦX174-E (Fig. 4A).

Post-translational addition of SlyD to P-CF generated precipitates of ΦX174-E had no effect on its

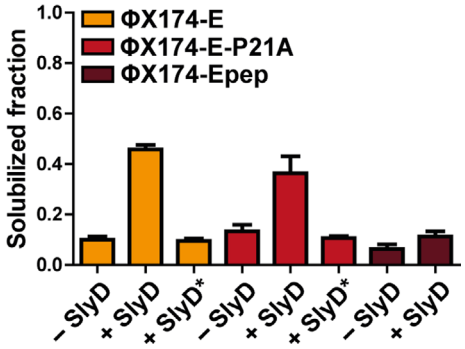

Fig. 3. Co-translational solubilization of CF synthesized ΦX174-E derivatives with SlyD. ΦX174-E derivatives containing a C-terminal StrepII-tag were synthesized in BL21(DE3)ΔSlyD/X lysate with/without 100 μM SlyD or 100 μM of the isomerization inactive mutant SlyD*. After expression, the fraction of solubilized ΦX174-E derivatives was determined via immunoblotting of supernatant and pellet using α-StrepII antibodies. The combined signal from pellet and supernatant was normalized to 1. Columns represent means of $n = 6$ independent CF reactions. In case of ΦX174-E-P21A with SlyD, the number of biological repeats equals $n = 12$. Error bars indicate the SEM.

solubilization (data not shown). Furthermore, the post-translational interaction of SlyD with D-CF synthesized ΦX174-E or with ΦX174-E already inserted/associated with NDs was tested. ΦX174-E was co-translationally solubilized by either NDs (DMPG) or detergent micelles by synthesis in the presence of 0.4% Brij35. The solubilized ΦX174-E was immobilized on magnetic beads by its StrepII-tag, and purified SlyD was added to analyze possible complex formation. However, a pulldown of SlyD was neither possible with ΦX174-E in NDs nor with ΦX174-E in detergent. This indicates that SlyD may only interact with nascent ΦX174-E and does not bind to ΦX174-E already solubilized in either detergent

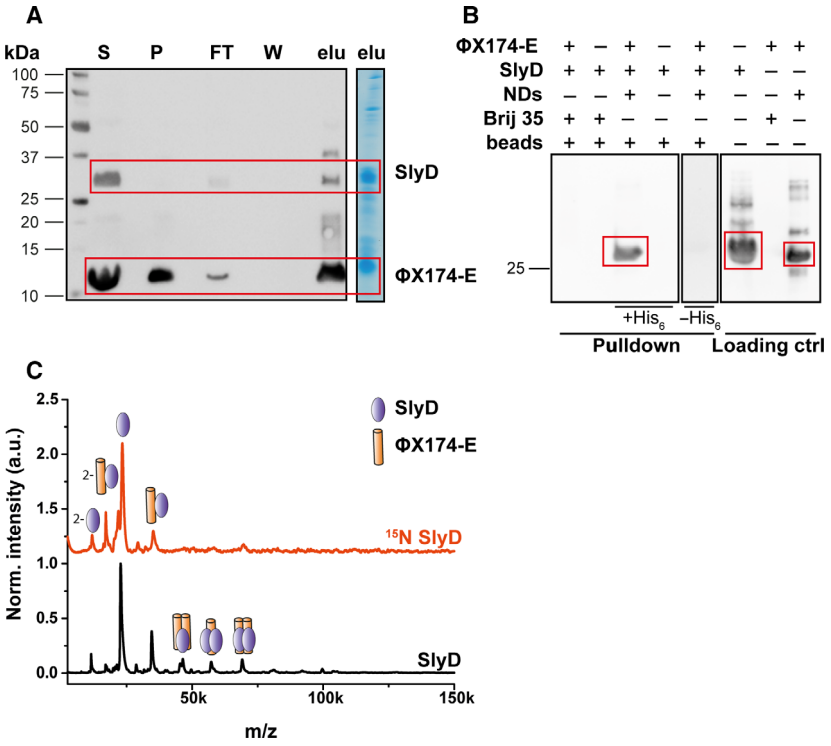

Fig. 4. Co-translational versus post-translational complex formation of ΦX174-E with SlyD. (A) Co-translational complex formation of ΦX174-E with SlyD. ΦX174-E was CF (A19 lysate) synthesized in the presence of supplied 100 μM SlyD. Supernatant (S) and precipitate (P) were separated, and ΦX174-E was purified from the supernatant by affinity chromatography via its StrepII-tag and analyzed by SDS/PAGE and immunoblotting. Proteins were detected with α-His-tag and α-StrepII-tag antibodies. FT, flow through; W, wash fraction; elu, elution fraction. The right panel shows a Coomassie Brilliant Blue-stained SDS/PAGE of the elution fraction. SlyD co-purifies with ΦX174-E. The data show a representative purification of the complex. (B) Post-translational interaction of purified ΦX174-E with SlyD was analyzed in pulldown assays. ΦX174-E was synthesized in the presence of either NDs (with or without His_6-tag) or of the detergent Brij35 and immobilized by its C-terminal StrepII-tag. SlyD was used as prey protein to analyze putative binding. Potentially bound SlyD was detected by immunoblotting with α-His-tag antibodies. The first panel shows samples of SlyD with ΦX174-E in Brij35 and NDs containing a His-tag, as well as the corresponding SlyD controls without immobilized ΦX174-E. No pulldown of SlyD is detectable with both ΦX174-E samples. The detected band in lane 3 corresponds to MSP1E3D1 also carrying a His-tag. Controls with NDs assembled with MSP1E3D1 without a His-tag did not give a signal (second panel). The third panel displays the controls SlyD and immobilized ΦX174-E in detergent and NDs. The immunoblot shows a representative result of $n = 3$ independently performed biological repeats. (C) LILBID-MS analysis of the purified ΦX174-E/SlyD complex. Pictograms in mass spectra illustrate assigned complexes. Charge states are indicated if they differ from 1-. ΦX174-E is present as monomer and dimer. To verify the peak assignments, corresponding spectra from complexes containing ^{15}N-labeled SlyD were taken (red line). All assigned peaks showed the expected mass shift.

or NDs (Fig. 4B). The purified co-translationally formed ΦX174-E/SlyD complex was further analyzed by native LILBID mass spectrometry and signals of 1 : 1, 1 : 2 and 2 : 2 complexes were observed (Fig. 4C).

SlyD interacts with the soluble domain of ΦX174-E

The incapability of SlyD to solubilize ΦX174-Epep indicated that the soluble domain of ΦX174-E could play a major role in the intermolecular interaction. This assumption was further analyzed with the construct GFP-Esol having the ΦX174-Epep domain deleted (Fig. 5). The GFP-Esol construct was hardly soluble and an estimate of 70% of the protein precipitated during CF expression. Yet, in the presence of 100 μM of either SlyD or SlyD*, the amount of soluble GFP-Esol was more than doubled (Fig. 5A,B). To exclude an influence of the fusion protein on the interaction, a control of GFP alone was expressed and addition of SlyD did not entail solubility increase or unspecific binding (Fig. 5C,D). The data imply that the SlyD P-domain function has only a minor role in the complex formation with ΦX174-E. Similar to SlyD/ΦX174-E, a stable complex was formed with SlyD and GFP-Esol that could be purified by affinity chromatography (Fig. 5E). Native LILBID mass

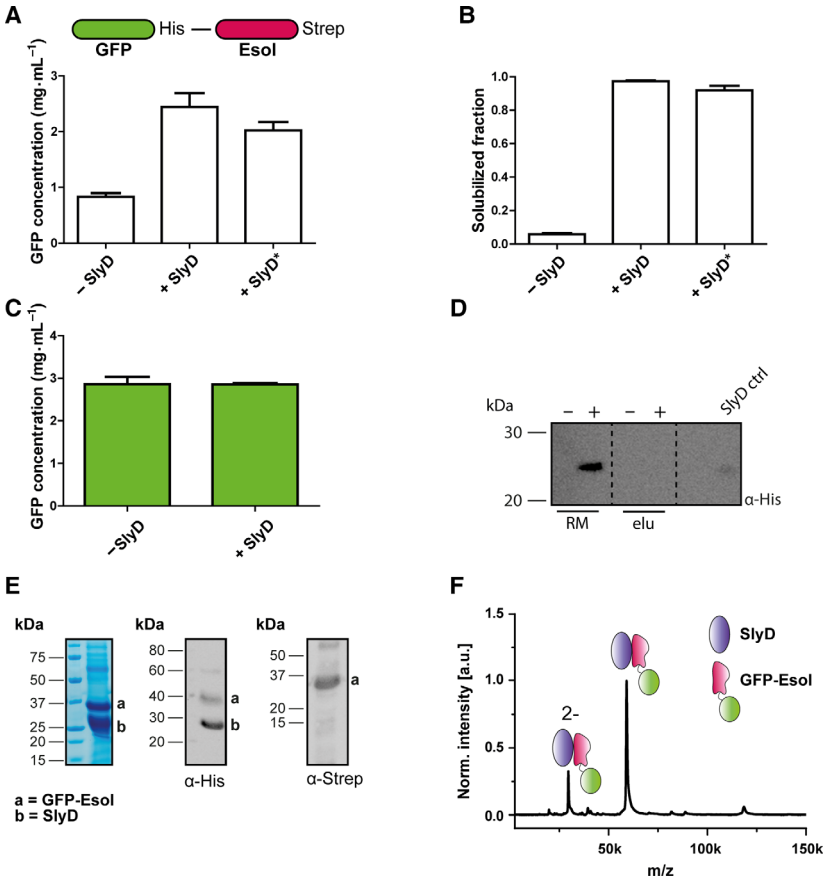

Fig. 5. SlyD interacts with the soluble domain of ΦX174-E. (A) GFP-Esol was synthesized in A19 S30 lysate in the absence and presence of 100 μM SlyD or SlyD*, and GFP fluorescence was measured in the soluble fraction. The solubility of GFP-Esol was increased in the presence of both, SlyD and SlyD*. The pictogram illustrates the GFP-Esol construct. Error bars represent the SEM of fluorescence measurements from $n = 6$ independent biological repeats for 0 μM SlyD and 100 μM SlyD* and $n = 5$ for 100 μM SlyD. (B) Immunodetection of GFP-Esol in the supernatant after synthesis in the presence of 100 μM SlyD or SlyD*. The proteins were synthesized in BL21(DE3)ΔSlyD/X S30 lysate. The combined signal from pellet and supernatant was normalized to 1. Columns represent means of $n = 6$ independent CF reactions. Error bars indicate the SEM. (C) To analyze the effect of SlyD addition to the CF expression of GFP, 100 μM SlyD were added to the CF reaction and the final GFP concentration in the supernatant was quantified via fluorescence measurement. Addition of SlyD to the reaction did not result in increased GFP amounts or solubility. Error bars indicate the SEM of fluorescence measurements from $n = 6$ biological repeats for GFP alone and $n = 3$ for GFP with 100 μM SlyD. (D) GFP was purified from the RM via its StrepII-tag, and the sample was analyzed for co-purified SlyD by immunoblotting. SlyD is present in the unpurified RM (left panel (RM), +), but does not co-purify with GFP (middle panel (elu), +). Purified SlyD was used as loading control (right panel). The SDS/PAGE shows a representative purification result. (E) Typical copurification of SlyD with GFP-Esol via the StrepII-tag of GFP-Esol. The two proteins are visible in the elution fraction after SDS/PAGE by Coomassie Brilliant Blue staining (left panel) and after immunoblotting with α-His antibodies (middle panel). The right panel illustrates the immunodetection of GFP-Esol in the sample by α-StrepII antibodies. (F) LILBID-MS analysis of the purified GFP-Esol/SlyD complex indicating a 1 : 1 ratio of the two proteins. Pictograms illustrate the assigned complexes for each peak. Charge states are indicated if they differ from 1-.

spectrometry analysis revealed the formation of a 1 : 1 complex of the two proteins (Fig. 5F).

Membrane insertion of ΦX174-E is restricted by the P21 residue and by its soluble domain

We further analyzed the effect of SlyD interaction on membrane association/insertion of ΦX174-E derivatives. The proteins were CF synthesized in the presence of 10 μM NDs and increasing concentrations of SlyD (Fig. 6). According to Fig. 2, NDs are limiting at 10 μM for the solubilization of ΦX174-E and effects of SlyD are more pronounced. While solubilization of ΦX174-E with NDs in the absence of SlyD was very low, increasing SlyD concentrations resulted in strongly improved solubilization (Fig. 6A). The basic solubilization of

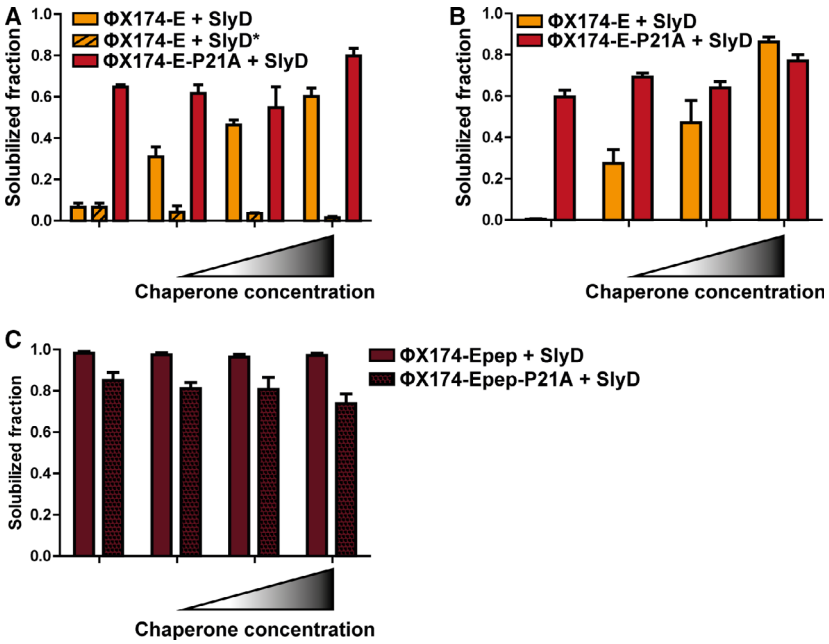

Fig. 6. Solubilization and membrane insertion of ΦX174-E derivatives in the presence of SlyD and NDs. CF reactions containing 10 μM NDs (DMPG) were supplied with increasing SlyD or SlyD* concentrations of 0, 10, 30 and 100 μM. Solubilization and ND insertion efficiencies of the synthesized ΦX174-E derivatives containing a C-terminal StrepII-tag were determined by quantifying pellet and supernatant fractions via immunoblotting using α-StrepII antibodies. The combined signal from pellet and supernatant was normalized to 1. The error bars represent the SEM. (A) Expression of ΦX174-E and the mutant ΦX174-E-P21A with SlyD ($n = 6$) or with the inactive mutant SlyD*($n = 3$). CF reactions were performed with A19 S30 lysate. (B) Expression of ΦX174-E ($n = 6$ for all conditions except for 0 μM SlyD, where $n = 5$) and ΦX174-E-P21A ($n = 6$) with SlyD in BL21(DE3)ΔSlyD/X S30 lysate. (C) Expression of ΦX174-Epep and ΦX174-Epep-P21A with SlyD in BL21(DE3) ΔSlyD/X S30 lysate ($n = 6$).

ΦX174-without SlyD could be completely abolished by using CF lysates from strain BL21(DE3)ΔSlyD/X (Fig. 6B). This verifies that some residual SlyD in the standard A19 lysates is active to solubilize ΦX174-E. Reduction of this residual ΦX174-E solubilization with increasing concentrations of SlyD* may indicate formation of nonproductive SlyD complexes.

It has to be considered that the solubilization of ΦX174-E in the presence of high SlyD concentrations in this experiment does not yet indicate the association/insertion of ΦX174-E into the provided NDs as SlyD/ΦX174-E complexes are already soluble without NDs (Fig. 3). In contrast, efficient solubilization of the lysis-deficient mutant ΦX174-E-P21A in the absence of SlyD indicates a SlyD-independent mechanism. Even at the highest concentration of 100 μM, addition of SlyD showed only a minor effect on solubilization of ΦX174-E-P21A (Fig. 6A,B). The conformation of the P21 peptidyl-proline linkage is thus likely a bottleneck for efficient membrane insertion of ΦX174-E. However, as shown in Fig. 3, SlyD still efficiently binds to ΦX174-E-P21A and can keep it soluble. Similar to ΦX174-E-P21A, the truncated derivatives ΦX174-Epep and ΦX174-Epep-P21A were readily solubilized with the provided NDs independently of SlyD (Fig. 6C). These results indicate that the soluble domain of ΦX174-E in combination with the P21 residue has a critical effect on membrane insertion of the toxin.

Oligomeric assembly of ΦX174-E constructs in ND membranes or detergent environment

The estimated ND to protein ratios from the solubilization kinetics indicates the insertion of multiple copies of ΦX174-Epep and probably also of ΦX174-E into one ND. However, it remains unclear whether multiple inserted monomers assemble into an oligomeric complex. Native LILBID mass spectrometry provides an excellent tool to identify oligomeric states of membrane proteins in NDs [21,28]. Carefully tuning the energy of the laser beam can result into partial sample dissociation. Complexes that lose their scaffold proteins are especially helpful, because they are considered stable. The largest protein complex detected without scaffold proteins in the resulting spectrum represents the biggest complex formed in the ND, or at least a stable subcomplex of the sample. Any smaller detected oligomeric forms may also exist or may be

caused by laser-induced dissociation. The ΦX174-Epep and ΦX174-E proteins were CF synthesized in the presence of 10 μM NDs but at first without SlyD. The solubilized fractions of the two proteins were purified via their C-terminal StrepII-tags and analyzed by LILBID mass spectrometry (Fig. 7). Only monomers were detected with wild-type ΦX174-E in association with NDs (Fig. 7A(iii)). In contrast, for ΦX174-Epep samples, the spectra revealed a pattern of oligomeric assemblies of up to hexamers (Fig. 7B(ii)). Interestingly, the trend of ΦX174-Epep to oligomerize was stronger in detergent after D-CF expression and up to dodecameric complexes were observed (Fig. 7B(i)). For ΦX174-E, still only monomers were detectable in detergent (Fig. 7A(i)).

If ΦX174-E is synthesized in the presence of both, supplied NDs and SlyD, oligomeric complexes of up to hexamers are formed (Fig. 7A(iv)). The complexes are clearly stable as they can be observed in the mass spectra even after loss of the scaffold proteins. Furthermore, despite purification of the ΦX174-E/ND complex via the StrepII-tag of ΦX174-E, SlyD is still detectable in the sample. In detergent ΦX174-E, monomers and dimers were observed (Fig. 7A(ii)), but no higher oligomers. Both conformations were still attached to SlyD.

Next, we analyzed the effect of the P21 residue on the oligomerization of ΦX174-E. Spectra of purified ΦX174-E-P21A/ND complexes revealed only monomeric ΦX174-E-P21A, regardless of the presence or absence of SlyD (Fig. 7C(ii) and (iii)). Similarly, only ΦX174-E-P21A monomers were detectable in detergent (Fig. 7C(i)). In contrast, the P21A mutation had no negative effect on the oligomerization efficiency of ΦX174-Epep and up to decameric assemblies were observed (Fig. 7D).

Oligomerization of ΦX174-E may result in the formation of pores in the membrane. To test this hypothesis, we took advantage of a recently developed technique to fuse ND membranes with other membranes provided in *trans* resulting in the transfer of ND inserted membrane proteins [33]. Liposomes filled with carboxyfluorescein were prepared and released fluorescence was measured after incubation with ΦX174-E/ND, ΦX174-Epep/ND or ΦX174-E-P21A/ND complexes (Fig. 7E,F). Successful transfer of the complexes by fusion of the ND membranes with the liposomes could result into pore formation followed by carboxyfluorescein efflux and fluorescence increase in the supernatant of the assay. A significant increase in carboxyfluorescein efflux was measured in assays with ΦX174-E compared to the lysis-deficient ΦX174-E-P21A and ΦX174-Epep derivatives (Fig. 7F).

Membrane delivery of ΦX174-E from ΦX174-E/SlyD complexes

We speculate that the binding and solubilization by SlyD results in a ΦX174-E conformation competent for membrane insertion. The high stability of the ΦX174-E/SlyD complex further gives evidence that membrane insertion does not necessarily need to be coordinated with the translation process and might also happen post-translationally. We therefore analyzed whether ΦX174-E can be transferred into empty ND membranes from a purified ΦX174-E/SlyD complex. Purified ΦX174-E/SlyD complexes were incubated with NDs for a period of 12 h and then again purified by the StrepII-tag of ΦX174-E (Fig. 8). The elution fraction of this purification was then applied to a further IMAC purification to capture residual SlyD protein. The presence of the scaffold protein MSP in the elution fraction of the StrepII purification indicates an association of ΦX174-E with NDs. After subsequent IMAC purification, the majority of ΦX174-E and MSP is present in the flow-through fraction, thus indicating a transfer of ΦX174-E into NDs. Some remaining SlyD is still detectable in the flow-through fraction, as well. The residual co-elution of SlyD may result from samples present in some interim processes, or it could indicate that some chaperone still stays attached to ΦX174-E after membrane delivery.

Discussion

Lysis activity of wild-type ΦX174-E strictly depends on the cytoplasmic chaperone SlyD, a bi-functional protein in *E. coli* containing a peptidyl-prolyl *cis-trans* isomerase domain and an integrated IF domain with general chaperone activity [12,34]. CD spectroscopy did not reveal evidence of a ΦX174-Epep conformational change upon incubation with SlyD post-translationally [14]. Yet, three of the five peptidyl-prolyl bonds of ΦX174-E are in its transmembrane domain and the residue P21 is absolutely essential for lysis activity [8,30]. Isomerization of this or another proline residue by SlyD was therefore proposed to be a potential activation mechanism likely resulting in a conformational rearrangement of ΦX174-E. The lysis deficiency of ΦX174-E in *slyD* mutants was found to be associated with its failure to accumulate in the cell membrane [34]. It was further shown that SlyD stabilizes ΦX174-E and potentially protects it from proteolysis [13]. Replacement, but not deletion, of the soluble domain ΦX174-Esol with few selected unrelated proteins such as LacZ renders ΦX174-E lysis activity independent from SlyD and gives evidence that a certain

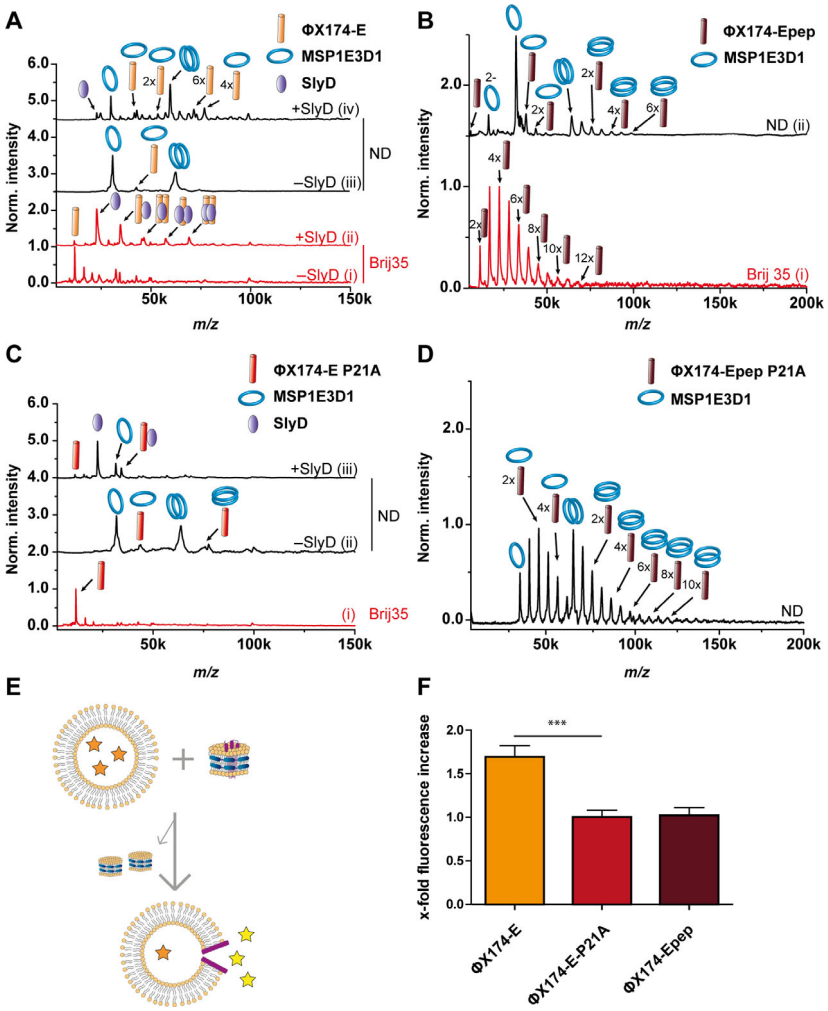

Fig. 7. Oligomeric assembly of ΦX174-E derivatives in NDs or detergent. (A–D) The constructs were CF expressed in the presence of 60 μM NDs (ΦX174-Epep) or 10 μM NDs (ΦX174-E) with DMPG (black lines) or in 0.4% of the indicated detergent (red lines). (A) ΦX174-E expressed with or without supplemented 100 μM SlyD. (B) ΦX174-Epep in NDs or Brij35 without SlyD. (C) ΦX174-E-P21A expressed in NDs or Brij35 in the presence and absence of 100 μM SlyD. (D) ΦX174-Epep-P21A in NDs without SlyD supplementation. Pictograms illustrate all components which constitute the complexes, which were assigned to the respective peaks. If charged states differed from −1, they are indicated. For clarity, assignment of only relevant peaks is shown. Laser intensities were adjusted between 10 and 20 mJ in order to optimize ion yield while preserving high-order complexes. (ΦX174-Epep in NDs 10 mJ and in Brij35 18 mJ; ΦX174-E 10 mJ; ΦX174-E-P21A 18 mJ, ΦX174-Epep-P21A 20 mJ). (E) Illustration of the liposome lysis assay setup [33]. Carboxyfluorescein-filled liposomes are incubated with purified protein/ND complexes. Upon transfer of the proteins from ND to liposomal membranes, encapsulated carboxyfluorescein effluxes to the exterior and can be quantified by fluorescence measurements. (F) The effect of ΦX174-E as well as of nonlytic ΦX174-Epep and ΦX174-E-P21A on the integrity of liposomal membranes was analyzed. Control experiments were performed with empty NDs and defined as background fluorescence due to leakiness. The background fluorescence was subtracted and ΦX174-E-P21A values were normalized to 1. Error bars represent the SEM from $n = 4$ ($n = 3$ for ΦX174-Epep) independent biological repeats. An unpaired *t*-test ($P = 0.0007$) was used to determine statistical significance. Compared to its nonlytic derivatives, ΦX174-E shows increased carboxyfluorescence efflux after protein transfer.

length, structure or conformation of ΦX174-Esol, but not a particular sequence, might be essential [7,8,35]. SlyD-independent phenotypes can further be obtained by point mutations such as R3H and L19F in the N-terminal transmembrane domain of ΦX174-E [8,13].

Their hydrophobic character in combination with their bacteriolytic activity render ΦX174-E and similar toxins highly problematic for recombinant production in classical cell-based systems. By CF expression, toxic proteins can be synthesized and decent amounts of

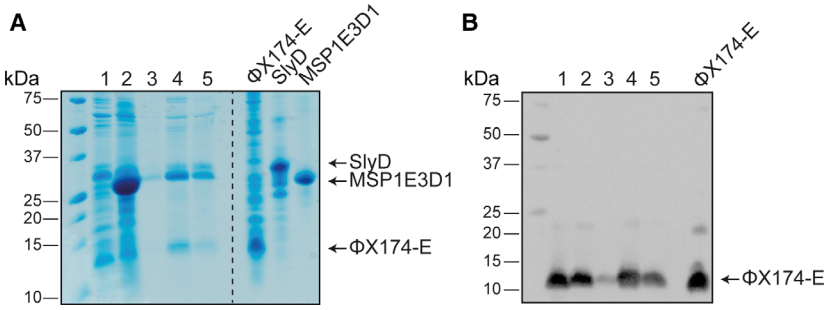

Fig. 8. Post-translational insertion of ΦX174-E into NDs. Samples were analyzed by SDS/PAGE. ΦX174-E/SlyD complexes (lane 1) purified via StrepII-tag were incubated 1 : 5 with NDs (DOPG + 20% cardiolipin) overnight at 16 °C (lane 2). The mixture was first purified by the StrepII-tag of ΦX174-E and then subjected to an IMAC purification. Lane 3, elution from Strep-purification indicating co-eluting MSP1E3D1; lane 4, concentrated flow through from IMAC purification; lane 5, concentrated elution from IMAC purification. P-CF expressed ΦX174-E, as well as purified SlyD and MSP1E3D1 were loaded as controls. FT and elu fraction of the IMAC purification contain all three proteins in different ratios. (A) Coomassie Brilliant Blue staining; (B) Immunoblotting with α-StrepII antibodies identifying ΦX174-E in all samples. The data show a representative result of $n = 3$ independently performed biological repeats.

ΦX174-E and derivatives were produced. The obtained data support a refined model of ΦX174-E activation by SlyD (Fig. 9). We propose an intramolecular interaction of the two ΦX174-E domains resulting in an auto-inhibitory complex, while SlyD is competing with the interface formation. The described SlyD independent but still lytic mutations R3H and L19F in the ΦX174-E transmembrane domain could thus be core residues in the interface of the suggested auto-inhibitory complex [8,13]. Once the inactive conformation of ΦX174-E is formed, interaction with SlyD is no longer possible. This explains the incapability to detect a post-translational interaction of SlyD with ΦX174-E solubilized in NDs or in detergents. The P21A mutation and the resulting structural changes in the transmembrane domain of ΦX174-E-P21A prevent formation of the auto-inhibitory complex and the synthesized mutant protein thus readily inserts into ND membranes. Membrane insertion of ΦX174-E-P21A is SlyD independent, although the mutant protein can form a stable complex with SlyD. Interestingly, only wild-type SlyD but not the P-domain defective SlyD* formed a stable complex with ΦX174-E-P21A or ΦX174-E. An initial contact of the SlyD P-domain, presumably with the nascent transmembrane domain of full-length ΦX174-E derivatives is therefore necessary to form stable soluble complexes. If formation of this contact is not possible as in case of SlyD*, synthesized full-length ΦX174-E derivatives will instantly precipitate. While the P21 residue in ΦX174-E is obviously dispensable for this contact, it does require a functional SlyD P-domain. We assume that the initial interaction of the SlyD P-domain with the transmembrane domain of ΦX174-E is either relatively weak or transient as the ΦX174-Epep construct could not be solubilized by SlyD. This is in agreement with previous reports that failed to detect an interaction of SlyD with a synthetic ΦX174-Epep construct by CD spectroscopy [14].

In contrast, SlyD binds strongly to the soluble domain ΦX174-Esol and the SlyD complexes formed with nascent ΦX174-E, ΦX174-E-P21A, or GFP-Esol were sufficiently stable to be purified. Based on the obtained results, we propose a sequential two-step interaction model of SlyD with ΦX174-E (Fig. 9). In a first and rather weak or transient contact, the transmembrane domain of ΦX174-E is bound by the P-domain of SlyD. While a direct proof is still missing, this interaction might result in an isomerization of the P21 residue, accompanied by an intramolecular switch and leading to a membrane insertion competent conformation of ΦX174-E. As the affinity of this contact appears to be low, an excess of SlyD is necessary to keep substantial amounts of synthesized ΦX174-E in solution. In a second step, the complex is stabilized by interaction of the ΦX174-E soluble domain with SlyD, presumably via its IF domain. Such conformational regulation mechanisms are relatively frequent in nature [36]. The infection process of *E. coli* cells by the filamentous phage fd is initiated by the *cis-trans* isomerization of a specific proline residue in the surface exposed phage gene-3 protein [37]. In the ΦX174 infection process, SlyD may act as accessory cellular factor to modulate the suggested ΦX174-E auto-inhibition and to initiate lysis onset. This supports the proposed biological role of the SlyD interaction as quorum sensing monitor to initiate cell lysis preferentially at optimal growth conditions of infected bacteria [6,13].

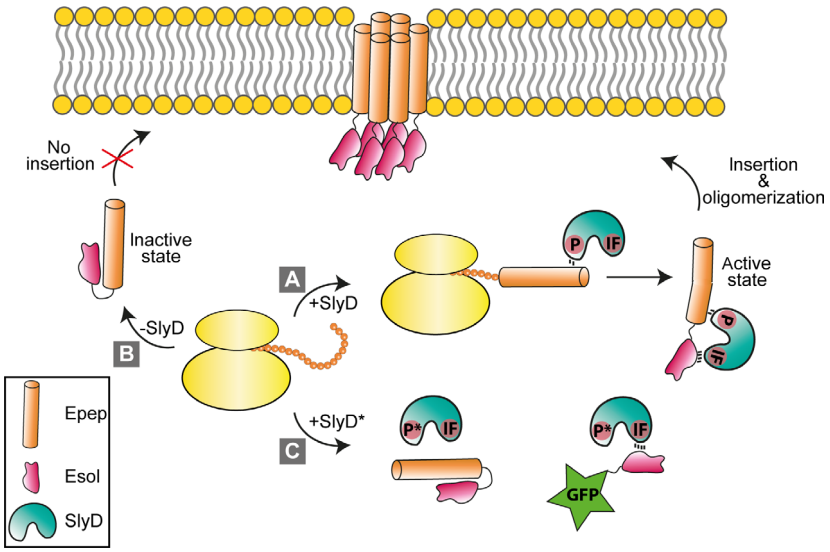

Fig. 9. Proposed mechanism of SlyD catalyzed membrane insertion of ΦX174-E. (A) In the presence of functional SlyD, the SlyD P-domain can interact with the nascent ΦX174-Epep domain. Upon completion of translation, the SlyD IF domain further interacts with the ΦX174-Esol domain thus forming a stable SlyD/ΦX174-E complex. The SlyD solubilized ΦX174-E can then be delivered into the membrane and oligomerizes. (B) In the absence of SlyD, ΦX174-Epep interacts with ΦX174-Esol and a nonproductive intramolecular complex is formed. (C) The defective P-domain of SlyD* is unable to interact with nascent ΦX174-Epep and a nonproductive ΦX174-Epep/ΦX174-Esol complex is formed. However, the intact IF domain of SlyD* is still able to interact with ΦX174-Esol in the GFP-Esol construct.

A new detail in ΦX174-E function is the observed oligomer formation in the membrane. The detected complexes in NDs can be assumed to exist in natural membranes as well. With a variety of membrane proteins forming up to hexameric assemblies, we could previously demonstrate that ND membranes do not induce any artificial complex formations [21]. Nevertheless, the implemented ND membranes were empty and their lipid compositions were less complex than in native bacterial cell membranes. Furthermore, physical characteristics of ND membranes such as curvature or lipid mobility are different from cell membranes and potential subtle effects of these parameters on ΦX174-E behavior in membranes could still be possible. Oligomerization of ΦX174-E is directed by the transmembrane domain, providing the interface for assembly. The role of the P21 residue is still unclear. Oligomerization of ΦX174-Epep as well as of the mutant ΦX174-Epep-P21A indicates that P21 is dispensable for the homomeric assembly of the isolated transmembrane domain. Yet, oligomerization incapability of the mutant ΦX174-E-P21A demonstrates an additional effect of the soluble domain in homomeric assembly of the full-length toxin. Steric hindrance of ΦX174-Esol might prevent oligomer formation of ΦX174-E-P21A in the membrane, possibly by indirect interactions with the membrane. Secondary structure analysis predicts helical structures within ΦX174-Esol with a positively charged helix site that might be coordinated by the negatively charged membrane. The ΦX174-Esol domain has a relatively hydrophobic character. Synthesis as fusion to GFP resulted in mostly insoluble protein, unless SlyD was provided in excess to keep it soluble. The increased liposome leakage caused by ΦX174-E oligomers compared to ΦX174-Epep could indicate differences in the structure of the two assemblies. The ΦX174-E assembly obviously results in pore forming structures, which are not or less detectable with ΦX174-Epep or ΦX174-Epep-P21A assemblies. The ΦX174-Esol domain could therefore be somehow structurally integrated in the ΦX174-E membrane complex. Alternatively, constraints of the ΦX174-Esol domain might affect or slow down isomerization processes or conformational changes of the transmembrane domain in the full-length toxin. Constraints of covalently attached domains like ΦX174-Esol or even the unrelated LacZ might direct the P21 residue into a particular conformation rendering the transmembrane domain competent for oligomerization. This could explain the reported lysis activity of ΦX174-Epep-LacZ fusions [7,8,35].

The role of ΦX174-E oligomerization in bacterial cell lysis still deserves closer analysis in future. Loss of

oligomerization by the lysis-deficient ΦX174-E-P21A can be taken as first evidence of a potentially essential role in final toxicity. ΦX174-E binds to MraY via its transmembrane domain [11,38], while supporting effects in the SlyD mediated membrane integration cannot be ruled out. Also, assembly of higher ΦX174-E oligomers than the observed hexamers can currently not be excluded. Oligomerization could have been restricted by experimental conditions or by size of the implemented ND membranes. The observed oligomerization supports previous speculations about pore formation that would require high-order assemblies [4]. In a proposed three-stage lysis model, the soluble domain is translocated to the periplasmic space and pore formation is accompanied by oligomerization of the transmembrane domain or of both ΦX174-E domains [39]. A dual function of ΦX174-E by binding to MraY in addition to directly support pore formation might therefore still be considered. We could already show the functional CF synthesis of a variety of MraY proteins in combination with NDs [40]. The established CF expression platform of ΦX174-E now allows interaction studies of both proteins with detailed molecular and structural approaches.

In summary, the refined model proposes a dual and sequential interaction of SlyD with nascent ΦX174-E to transform the toxin into a membrane insertion competent conformation (Fig. 9). A first weak or transient interaction of the nascent transmembrane domain containing the P21 residue with the SlyD P-domain prevents toxin auto-inhibition and acts as quorum sensor for bacterial lysis. A second and more stable complex formation of ΦX174-Esol with the SlyD IF domain renders ΦX174-E structurally competent for membrane insertion. An essential role of the P21 residue could be to provide a suitable conformation for oligomerization of the full-length toxin in the membrane. Constraints of the attached soluble domain modulate adoption of the P21 conformation and some yet unknown mechanisms in final cell lysis. However, functional replacement of ΦX174-Esol by LacZ indicates that besides in the initial auto-inhibition mechanism, a specific interaction of ΦX174-Esol with the ΦX174-E transmembrane domain may no longer be required to reach the final lysis process.

Materials and methods

DNA techniques

The ΦX174-E gene was synthesized according to *E. coli* codon usage, and the first codon after the ATG start codon was changed to AAA (lysine) in some of the constructs for optimized CF expression [22]. All toxin constructs as well as a synthetic *slyD* gene (Eurofins Scientific GmbH, Frankfurt am Main, Germany) were cloned into the pET21a vector (Novagen, Darmstadt, Germany) containing either a C-terminal StrepII-tag or in case of SlyD a His_{10}-tag. GFP-Esol contains a His_6-tag following the GFP sequence and a C-terminal StrepII-tag. The inserts were PCR amplified and inserted into the vector by using the restriction enzymes *NdeI*/*KpnI*, *NdeI*/*XhoI* in case of *slyD* or *BamHI*/*XhoI* for GFP-Esol. Point mutations for ΦX174-E-P21A and SlyD* (I42S, F132Y) were introduced by Quickchange PCR. All constructs and their characteristics are listed in Table 1. For co-expression with ΦX174-E, *slyD* was amplified from *E. coli* chromosomal DNA and cloned into the vector pRSFDuet-1 (Novagen) with *NdeI*/*XhoI*.

CF protein expression and ND preparation

For general CF expression, a continuous exchange system based on A19 *E. coli* S30 lysates was used. CF expression, S30 lysate and T7 RNA polymerase preparation were performed as described elsewhere [18,23,24]. Effects of supplied SlyD were analyzed with SlyD deficient BL21(DE3) ΔSlyD/X S30 lysates [25]. For analytical scale expressions, a reaction mix (RM) to feeding mix ratio of 1 : 15 with a previously determined Mg^{2+} ion optimum of 20 mM was used. All constructs were expressed in either the precipitate forming (P-CF), the detergent based (D-CF) or the lipid based (L-CF) mode. In the D-CF mode, the reaction was adjusted to 0.4% of the indicated detergent.

For ND preparation, the MSP1E3D1 scaffold protein was expressed as previously described [26]. Protein to lipid concentrations of 1 : 110 for 1,2-dimyristoyl-sn-glycero-3-phospho-(1'-rac-glycerol) (DMPG), 1 : 115 for 1,2-dimyristoyl-sn-glycero-3-phosphocholine (DMPC), 1 : 80 for 1,2-dioleoyl-sn-glycero-3-phospho-(1'-rac-glycerol) (DOPG) and 1 : 90 for 1-palmitoyl-2-oleoyl-sn-glycero-3-phospho-(1'-*rac*-glycerol) (POPG) were mixed with 0.1% (w/v) n-dodecyl phosphocholine (DPC) in DF buffer (10 mM Tris/HCl pH 8.0, 100 mM NaCl) and dialyzed 3× over night against DF buffer at room temperature for detergent removal. Subsequently, NDs were centrifuged to remove aggregates and concentrated using Centriprep devices (Merck Millipore, Darmstadt, Germany, 10 kDa MWCO) to a final concentration of 500–1000 μM.

SlyD expression and IMAC purification

Escherichia coli T7 express cells (New England Biolabs, Frankfurt am Main, Germany) were transformed with the *slyD* carrying plasmid. Expression was carried out in Luria Broth (LB) medium supplemented with 100 $\mu g \cdot mL^{-1}$ ampicillin. Protein expression was induced at OD_{600} of 0.6 with 1 mM IPTG, followed by further 3 h growth at 37 °C. For SlyD purification, cells were resuspended in purification

buffer (50 mM sodium phosphate pH 7.0, 300 mM NaCl), disrupted by sonication and centrifuged to remove cell debris. The lysate was filtrated and loaded on Ni^{2+}-NTA agarose (Qiagen, Hilden, Germany) pre-equilibrated with purification buffer. The column was further washed with 5 column volumes (cv) of purification buffer, 5 cv purification buffer containing 50 mM imidazole and protein was eluted with 2 cv purification buffer supplemented with 300 mM imidazole. To obtain homogeneous protein, size exclusion chromatography was performed on a Superdex 75 10/300 GL column. Purified SlyD was concentrated using ultrafiltration (Amicon Ultra, Merck Millipore, 10 kDa MWCO).

SDS/PAGE and immunoblotting

P-CF synthesized proteins were resuspended in a volume of S30C buffer (10 mM Tris acetate pH 8.2, 14 mM Mg $(OAc)_2$, 60 mM KOAc) equal to the RM volume. Protein samples were mixed with SDS loading buffer (100 mM Tris/HCl pH 6.8, 8 M urea, 20% (w/v) SDS, 20% (v/v) β-mercaptoethanol, 15% (v/v) glycerol, 0.12% (w/v) bromphenol blue), denatured at 95 °C and separated on discontinuous 4–11% Tris-tricine-SDS gels. Protein stacking was performed at 90 V and separation was carried out at 150 V. Following SDS/PAGE, the gels were either fixated in a 50% (v/v) ethanol and 10% (v/v) acetic acid solution and stained with colloidal staining solution (0.02% (w/v) Coomassie Brilliant Blue G250, 5% (w/v) aluminum sulfate-(14-18)-hydrate, 10% (v/v) ethanol, 2% (v/v) orthophosphoric acid) or used for immunoblotting.

In case of immunoblotting, a wet transfer western blotting system was used. Following SDS/PAGE, proteins were blotted on a methanol activated 0.45 μM PVDF membrane at 340 mA for 35 min in Towbin buffer (25 mM Tris/HCl pH 8.3, 192 mM glycine, 15% (v/v) methanol). The membrane was blocked with 4% (w/v) skim milk powder in PBS-T (2.6 mM KCl, 1.8 mM KH_2PO_4, 137 mM NaCl, 10 mM Na_2HPO_4, 0.05% (v/v) Tween-20) for 1 h at room temperature, followed by antibody incubation (α-StrepII-HRP, 1 : 7000 dilution in 0.5% skim milk powder in PBS-T) for 1 h at room temperature. In case of the α-His antibody a dilution of 1 : 2000 was used. Following 1-h incubation at room temperature, the membrane was washed three times with PBS-T and incubated with α-mouse-HRP (1 : 5000) in 0.5% skim milk powder in PBS-T for 1 h at room temperature or at 4 °C over night. After subsequent washing with PBS-T, the membrane was analyzed by chemiluminescence detection.

LILBID mass spectrometry

All protein samples were buffer exchanged prior to MS analysis using Zeba Micro Spin desalting columns (Thermo Scientific, Dreieich, Germany, 7 kDa MWCO). ND samples were buffer exchanged to 50 mM ammonium acetate pH 7.4, whereas detergent solubilized samples were buffer exchanged to 50 mM Tris/HCl pH 8.0 with 0.02% Brij 35. 4 μL of buffer exchanged sample was used for each measurement.

A piezo-driven droplet generator (MD-K-130, Microdrop Technologies GmbH, Norderstedt, Germany) was used to produce sample droplets of 50 μm diameter with a frequency of 10 Hz at 100 mbar. The droplets were transferred to high vacuum and irradiated by an IR laser operating at 2.94 μm. The pulse energy of the laser was varied within a range of 10–23 mJ. Droplet irradiation leads to an explosive expansion, releasing the solvated analyte ions. Ions were accelerated by a pulsed electric field and were analyzed with a homebuilt time-of-flight setup including a reflectron operating at 10^{-6} mbar. Further information regarding LILBID mass spectrometry has been previously published in detail [27,28]. Ion detection was carried out in the negative ion mode. Data acquisition was done using a homebuilt software based on LabView and spectra processing was performed using the software MASSIGN [29]. The shown mass spectra are averaged signals of 1000 droplets.

In vivo toxicity

Escherichia coli Lemo21 (DE3) containing appropriate combinations of the vectors pET21-ΦX174-E and pRSF-Duet-1-SlyD were incubated overnight at 37 °C in LB medium to produce the starter culture. If appropriate, the culture was supplemented with final concentrations of 100 $\mu g \cdot mL^{-1}$ ampicillin, 30 $\mu g \cdot mL^{-1}$ chloramphenicol or 500 $\mu g \cdot mL^{-1}$ L-rhamnose. The next day, 12 mL expression culture supplemented with appropriate antibiotics and a final concentration of 500 $\mu g \cdot mL^{-1}$ L-rhamnose was inoculated with 120 μL of the starter culture at 37 °C and 180 rpm. Cultures were adjusted to 500 μM IPTG at $OD_{600} \sim 0.4$ (t = 0) to induce expression of ΦX174-E in the absence/presence of SlyD. The effect of ΦX174-E overexpression in the absence/presence of the chaperone or L-rhamnose was monitored by measuring the OD_{600} in 30 min intervals. All measurements were done in triplicates.

StrepII-Tactin purification of CF expressed toxins

For purification of StrepII-tagged proteins, the required amount of StrepII-Tactin resin (iba, Göttingen, Germany) was equilibrated with 10 cv of Strep-binding buffer (100 mM Tris/HCl pH 8.0, 100 mM NaCl). For 100 μL RM approximately 150 μL resin was used. The RM containing the protein of interest was diluted in a 1 : 3 ratio in Strep-binding buffer and re-loaded 4 times using gravity flow columns. After washing with 5 cv Strep-binding buffer the protein was eluted with 2× 1 cv elution buffer (Strep-binding buffer containing 15 mM d-desthiobiotin). Subsequently the proteins were concentrated using ultrafiltration (Amicon Ultra, Merck Millipore, 10 kDa MWCO).

SlyD pulldown

For StrepII pulldown assays, MagStrep 'type3' XT beads (iba) were used. For each reaction, 85 μL of a 5% suspension was washed three times with H_2O and equilibrated in either Strep-binding buffer or Strep-binding buffer supplemented with 0.02% Brij35. 50 μg of ΦX174-E in either detergent or ND membranes were immobilized by incubating the beads with the protein for 1 h at 4 °C in an overhead shaker. To remove unbound protein, beads were washed 3× with Strep-binding buffer. 50 μg SlyD in Strep-binding buffer were added to the immobilized bait protein and incubated for 4 h at 4 °C in an overhead shaker for binding. Subsequently, the beads were washed 3× with Strep-binding buffer to remove unbound SlyD and proteins were eluted by addition of 40 μL of SDS loading buffer and sample heating for 10 min at 75 °C.

Fluorescence-based liposome assay

10 mg of DOPG phospholipids was dissolved in 1 mL of chloroform and dried in a round bottom flask. The dried lipids were resuspended in 1 mL of CF buffer (50 mM 5,6-carboxyfluorescein, 5 mM Hepes pH 8.0) in a sonication bath until the suspension became clear. The preparation was passed through 5 freeze and thaw cycles and extruded through filters with a pore diameter of 200 nm to obtain liposomes of monodisperse size. To exchange the liposome buffer, liposomes were pelleted at 100 000 ***g*** for 30 min and resuspended in 5 mM Hepes pH 8.0. The procedure was repeated at least 3 times to remove residual carboxyfluorescein until the supernatant became clear.

For protein transfer from NDs into liposomes, 1 mg of carboxyfluorescein encapsulated liposomes was incubated with 5 μM of the previously purified protein/ND complex in 5 mM Hepes pH 8.0 for 90 min at 30 °C with slight shaking. As control, empty NDs were added to the liposomes. To separate liposomes from NDs, the mixture was centrifuged at 100 000 ***g*** for 30 min and the fluorescence of the supernatant fraction was monitored at (λ_{ex}. 492 nm, λ_{em}. 517 nm).

Post-translational transfer of ΦX174-E into NDs

For post-translational insertion into NDs, ΦX174-E/SlyD complexes were StrepII-purified, concentrated and the buffer was exchanged to Strep-binding buffer to remove d-desthiobiotin. In this particular setup, MSP1E3D1 with a removed His-tag was used. For optimal transfer rates DOPG NDs containing 20% cardiolipin were utilized. 100-μL reactions containing 100 μM NDs and 20 μM ΦX174-E/SlyD complexes were prepared and incubated over night at 16 °C in an overhead shaker. After incubation, the samples were centrifuged to remove possible precipitates and subjected to a StrepII-Tactin purification to remove empty NDs. Subsequently, an IMAC purification was conducted to separate remaining SlyD-bound ΦX174-E from ND inserted ΦX174-E. Potentially formed ΦX174-E/ND complexes were expected in the flow-through fractions.

Acknowledgements

We thank Vladimir Mokhonov for providing the strain BL21(DE3)ΔSlyD/X. We are grateful to Erik Henrich for helpful advice and discussions. We further thank Birgit Schäfer for technical assistance. Yi Ma was financially supported by Guangdong Natural Science Foundation (2019A1515011251), the Fundamental Research Funds for the Central Universities (2018MS54), and the opening fund of State Key Laboratory of Fermentation and Enzyme Engineering and China Scholarship Council (201706155087). Nina Morgner was funded by the Heisenberg Professor ERC starting grant. The work was further funded by the Collaborative Research Centre (SFB) 807 of the German Research Foundation (DFG), the state of Hessen (Center for Biomolecular Magnetic Resonance), and by the research training group Complex Light Control (CLiC) at the Goethe University Frankfurt.

Conflict of interest

The authors declare that the research was conducted in the absence of any commercial or financial relationships that could be construed as a potential conflict of interest.

Author contributions

JM and FB wrote the manuscript. Expression, protein purification, cloning, and method development were done by JM and YM. *In vivo* studies were performed by YM and JM. LILBID analysis was carried out by OP, JaM, and NM. FB, YM, and VD designed the project. All authors contributed to reading and approving the final version of the manuscript.

Peer Review

The peer review history for this article is available at https://publons.com/publon/10.1111/febs.15642.

References

1 Bernhardt TG, Wang IN, Struck DK & Young R (2002) Breaking free: "protein antibiotics" and phage lysis. *Res Microbiol* **153**, 493–501.
2 Young KD & Young R (1982) Lytic action of cloned ΦX174 gene E. *J Virol* **44**, 993–1002.

3 Witte A, Bläsi U, Halfmann G, Szostak M, Wanner G & Lubitz W (1990) PhiX174 protein E-mediated lysis of *Escherichia coli*. *Biochimie* **72**, 191–200.
4 Witte A, Wanner G, Bläsi U, Halfmann G, Szostak M & Lubitz W (1990) Endogenous transmembrane tunnel formation mediated by pX174 lysis protein E. *J Bacteriol Res* **172**, 4109–4114.
5 Witte A, Reisinger GR, Säckl W, Wanner G & Lubitz W (1998) Characterization of *Escherichia coli* lysis using a family of chimeric E-L genes. *FEMS Microbiol Lett* **164**, 159–167.
6 Chamakura K & Young R (2019) Phage single-gene lysis: finding the weak spot in the bacterial cell wall. *J Biol Chem* **294**, 3350–3358.
7 Maratea D, Young K & Young R (1985) Deletion and fusion analysis of the phage φX174 lysis gene E. *Gene* **40**, 39–46.
8 Tanaka S & Clemons WM Jr (2012) Minimal requirements for inhibition of MraY by lysis protein E from bacteriophage ΦX174. *Mol Microbiol* **85**, 975–985.
9 Bernhardt TG, Struck DK & Young R (2001) The lysis protein E of φX174 is a specific inhibitor of the MraY-catalyzed step in peptidoglycan synthesis. *J Biol Chem* **276**, 6093–6097.
10 Zheng Y, Struck DK & Young R (2009) Purification and functional characterization of ϕX174 lysis protein E. *Biochemistry* **48**, 4999–5006.
11 Rodolis MT, Mihalyi A, O'Reilly A, Slikas J, Roper DI, Hancock REW & Bugg TDH (2014) Identification of a novel inhibition site in translocase MraY based upon the site of interaction with lysis protein E from bacteriophage ϕX174. *ChemBioChem* **15**, 1300–1308.
12 Weininger U, Haupt C, Schweimer K, Graubner W, Kovermann M, Brüser T, Scholz C, Schaarschmidt P, Zoldak G, Schmid FX *et al*. (2009) NMR solution structure of SlyD from *Escherichia coli*: spatial separation of prolyl isomerase and chaperone function. *J Mol Biol* **387**, 295–305.
13 Bernhardt TG, Roof WD & Young R (2002) The *Escherichia coli* FKBP-type PPIase SlyD is required for the stabilization of the E lysis protein of bacteriophage φX174. *Mol Microbiol* **45**, 99–108.
14 Mendel S, Holbourn JM, Schouten JA & Bugg TDH (2006) Interaction of the transmembrane domain of lysis protein E from bacteriophage ΦX174 with bacterial translocase MraY and peptidyl-prolyl isomerase SlyD. *Microbiol* **152**, 2959–2967.
15 Chung BC, Zhao J, Gillespie RA, Kwon DY, Guan Z, Hong J, Zhou P & Lee SY (2013) Crystal structure of MraY, an essential membrane enzyme for bacterial cell wall synthesis. *Science* **341**, 1012–1016.
16 Jia B & Jeon CO (2016) High-throughput recombinant protein expression in *Escherichia coli*: current status and future perspectives. *Open Biol* **6**, 160196. https://doi.org/10.1098/rsob.160196
17 Yung MC, Bourguet FA, Carpenter TS & Coleman MA (2017) Re-directing bacterial microcompartment systems to enhance recombinant expression of lysis protein E from bacteriophage ϕX174 in *Escherichia coli*. *Microb Cell Fact* **16**, 71. https://doi.org/10.1186/s12934-017-0685-x
18 Henrich E, Dötsch V & Bernhard F (2015) Screening for lipid requirements of membrane proteins by combining cell-free expression with nanodiscs. *Method Enzymol* **556**, 351–369.
19 Roos C, Zocher M, Müller D, Münch D, Schneider T, Sahl HG, Scholz F, Wachtveitl J, Ma Y, Proverbio D *et al*. (2012) Characterization of co-translationally formed nanodisc complexes with small multidrug transporters, proteorhodopsin and with the *E. coli* MraY translocase. *Biochim Biophys Acta* **1818**, 3098–3106.
20 Harris NJ, Reading E, Ataka K, Grzegorzewski L, Charalambous K, Liu X, Schlesinger R, Heberle J & Booth PJ (2017) Structure formation during translocon-unassisted co-translational membrane protein folding. *Sci Rep* **7**, 8021. https://doi.org/10.1038/s41598-017-08522-9
21 Henrich E, Peetz O, Hein C, Laguerre A, Hoffmann B, Hoffmann J, Dötsch V, Bernhard F & Morgner N (2017) Analyzing native membrane protein assembly in nanodiscs by combined non-covalent mass spectrometry and synthetic biology. *eLife* **6**, e20954.
22 Haberstock S, Roos C, Hoevels Y, Dötsch V, Schnapp G, Pautsch A & Bernhard F (2012) A systematic approach to increase the efficiency of membrane protein production in cell-free expression systems. *Protein Expr Purif* **82**, 308–316.
23 Schwarz D, Klammt C, Koglin A, Löhr F, Schneider B, Dötsch V & Bernhard F (2007) Preparative scale cell-free expression systems: new tools for the large scale preparation of integral membrane proteins for functional and structural studies. *Methods* **41**, 355–369.
24 Reckel S, Sobhanifar S, Durst F, Löhr F, Shirokov VA, Dötsch V & Bernhard F (2010) Strategies for the cell-free expression of membrane proteins. *Methods Mol Biol* **607**, 187–212.
25 Mokhonov VV, Vasilenko EA, Gorshkova EN, Astrakhantseva IV, Novikov DV & Novikov VV (2018) SlyD-deficient *Escherichia coli* strains: a highway to contaminant-free protein extraction. *Biochem Biophys Res Commun* **499**, 967–972.
26 Denisov IG, Grinkova YV, Lazarides AA & Sligar SG (2004) Directed self-assembly of monodisperse phospholipid bilayer nanodiscs with controlled size. *J Am Chem Soc* **126**, 3477–3487.
27 Morgner N, Barth HD & Brutschy B (2006) A new way to detect noncovalently bonded complexes of

biomolecules from liquid micro-droplets by laser mass spectrometry. *Aust J Chem* **59**, 109–114.
28 Peetz O, Hellwig N, Henrich E, Mezhyrova J, Dötsch V, Bernhard F & Morgner N (2019) LILBID and nESI: different native mass spectrometry techniques as tools in structural biology. *J Am Soc Mass Spectrom* **30**, 181–191.
29 Morgner N & Robinson CV (2012) Massign: an assignment strategy for maximizing information from the mass spectra of heterogeneous protein assemblies. *Anal Chem* **84**, 2939–2948.
30 Witte A, Schrot G, Schön P & Lubitz W (1997) Proline 21, a residue within the α-helical domain of ΦX174 lysis protein E, is required for its function in *Escherichia coli*. *Mol Microbiol* **26**, 337–346.
31 Foshag D, Henrich E, Hiller E, Schäfer M, Kerger C, Burger-Kentischer A, Diaz-Moreno I, García-Mauriño SM, Dötsch V, Rupp S *et al.* (2018) The *E. coli* S30 lysate proteome: a prototype for cell-free protein production. *New Biotechnol* **40**, 245–260.
32 Zhang JW, Leach MR & Zamble DB (2007) The peptidyl-prolyl isomerase activity of SlyD is not required for maturation of *Escherichia coli* hydrogenase. *J Bacteriol* **189**, 7942–7944.
33 Patriarchi T, Shen A, He W, Baikoghli M, Cheng RH, Xiang YK, Coleman MA & Tian L (2018) Nanodelivery of a functional membrane receptor to manipulate cellular phenotype. *Sci Rep* **8**, 3556. https://doi.org/10.1038/s41598-018-21863-3
34 Suzuki R, Nagata K, Yumoto F, Kawakami M, Nemoto N, Furutani M, Adachi K, Maruyama T & Tanokura M (2003) Three-dimensional solution structure of an archaeal FKBP with a dual function of peptidyl prolyl cis–trans isomerase and chaperone-like activities. *J Mol Biol* **328**, 1149–1160.
35 Buckley KJ & Hayashi M (1986) Lytic activity localized to membrane-spanning region of ΦX174 E protein. *Mol Gen Genet* **204**, 120–125.
36 Pufall MA & Graves BJ (2002) Autoinhibitory domains: modular effectors of cellular regulation. *Annu Rev Cell Dev Biol* **18**, 421–462.
37 Eckert B, Martin A, Balbach J & Schmid FX (2005) Prolyl isomerization as a molecular timer in phage infection. *Nat Struct Mol Biol* **12**, 619–623.
38 Bernhardt TG, Roof WD & Young R (2000) Genetic evidence that the bacteriophage ΦX174 lysis protein inhibits cell wall synthesis. *Proc Natl Acad Sci USA* **97**, 4297–4302.
39 Schön P, Schrot G, Wanner G, Lubitz W & Witte A (1995) Two-stage model for integration of the lysis protein E of phi X174 into the cell envelope of *Escherichia coli*. *FEMS Microbiol Rev* **17**, 207–212.
40 Henrich E, Ma Y, Engels I, Münch D, Otten C, Schneider T, Henrichfreise B, Sahl HG, Dötsch V & Bernhard F (2016) Lipid requirements for the enzymatic activity of MraY translocases and *in Vitro* reconstitution of the lipid II synthesis pathway. *J Biol Chem* **291**, 2535–2546.